HHS Public Access

Author manuscript

J Mol Cell Cardiol. Author manuscript; available in PMC 2016 August 01.

Published in final edited form as:

J Mol Cell Cardiol. 2015 August ; 85: 1–12. doi:10.1016/j.yjmcc.2015.05.005.

Tbx5 and *Osr1* interact to regulate posterior second heart field cell cycle progression for cardiac septation

Lun Zhou[1,4], **Jielin Liu**[1], **Patrick Olson**[1], **Ke Zhang**[2], **Joshua Wynne**[3], and **Linglin Xie**[1,*]

[1]Department of Basic Sciences, School of Medicine and Health Sciences, University of North Dakota, Grand Forks, ND, 58202, USA

[2]Department of Pathology, School of Medicine and Health Sciences, University of North Dakota, Grand Forks, ND, 58202, USA

[3]Department of Internal Medicine, School of Medicine and Health Sciences, University of North Dakota, Grand Forks, ND, 58202, USA

[4]Department of Gerontology, Tongji Hospital, Huazhong University of Science and Technology, Wuhan, Hubei, 430030, China

Abstract

Rationale—Mutations of TBX5 cause Holt–Oram syndrome (HOS) in humans, a disease characterized by atrial or occasionally ventricular septal defects in the heart and skeletal abnormalities of the upper extremity. Previous studies have demonstrated that Tbx5 regulates *Osr1* expression in the second heart field (SHF) of E9.5 mouse embryos. However, it is unknown whether and how Tbx5 and Osr1 interact in atrial septation.

Objective—To determine if and how Tbx5 and Osr1 interact in the posterior SHF for cardiac septation.

Methods and Results—In the present study, genetic inducible fate mapping showed that *Osr1*-expressing cells contribute to atrial septum progenitors between E8.0 and E11.0. *Osr1* expression in the pSHF was dependent on the level of *Tbx5* at E8.5 and E9.5 but not E10.5, suggesting that the embryo stage before E10.5 is critical for Tbx5 interacting with Osr1 in atrial septation. Significantly more atrioventricular septal defects (AVSDs) were observed in embryos with compound haploinsufficiency for *Tbx5* and *Osr1*. Conditional compound haploinsufficiency for *Tbx5* and *Osr1* resulted in a significant cell proliferation defect in the SHF, which was associated with fewer cells in the G2 and M phases and a decreased level of *Cdk6* expression. Remarkably, genetically targeted disruption of *Pten* expression in atrial septum progenitors rescued AVSDs caused by *Tbx5* and *Osr1* compound haploinsufficiency. There was a significant decrease in *Smo*

*Please send correspondence to: Linglin Xie, MD, PhD, Department of Basic Sciences, University of North Dakota, School of Medicine and Health Sciences, 501 N. Columbia Rd, Rm 5741, Grand Forks, ND 58202-9037, Phone: 701-777-1320, linglin.xie@med.und.edu.

Conflict of interest statement: The authors declare that they have no conflict of interest.

expression, which is a Hedgehog (Hh) signaling pathway modulator, in the pSHF of *Osr1* knockout embryos at E9.5, implying a role for Osr1 in regulating Hh signaling.

Conclusions—Tbx5 and Osr1 interact to regulate posterior SHF cell cycle progression for cardiac septation.

Keywords

Tbx5; Osr1; atrioventricular septal defects (AVSDs); second heart field; cell cycle; Pten

Introduction

Atrial septation is the division of a common atrium into the left and right atria and is observed in a structurally mature four-chambered tetrapod heart. Atrial septal defects (ASDs) are one of the most common forms of human congenital heart diseases, affecting almost 1 child per 1,500 live births per year and make up 30% to 40% of all adult congenital heart diseases [1]. The atrial septum is formed by the atrioventricular endocardial cushions, the primary atrial septum, and the spina vestibuli or dorsal mesenchymal protrusion (SV/DMP), which undergo concurrent morphogenesis [2-8]. Failure to develop these distinct structures results in specific types of ASDs. Specifically, deficiency of the DMP results in primum ASDs, a type of atrioventricular septal defect (AVSD). Recent elucidation of the cellular sources of atrial septation has resulted in the identification of a role for second heart field (SHF) cardiac progenitors in atrial septation [9-14]. These studies demonstrate that progenitors of much, if not all, of the atrial septum, including the primary atrial septum (PAS) and SV/DMP, are SHF derivatives.

Long-standing genetic studies have shown that haploinsufficiency of GATA4, NKX2-5, and TBX5 causes ASDs in humans [15-18]. *Tbx5* is a member of the T-box transcription factor family and a key regulator of early cardiac morphogenesis; its importance is highlighted by the fact that haploinsufficiency of TBX5 causes Holt-Oram syndrome (HOS) in humans. HOS, characterized by forelimb deformities frequently combined with congenital heart defects [15, 17], is an autosomal-dominant disease, affecting one of every 100,000 live births. The majority of patients with HOS have cardiac defects, and ASDs occur in approximately half of those patients [19]. Tbx5 is known to interact with Nkx2-5 and Gata4 and to positively regulate transcription in the developing heart [16, 20]. Studies of Tbx5 in cardiac development have identified *Gja1, Gja5,* and *Nppa* as its target genes, but it is not known whether these targets regulate the development of the atrial septum [21, 22]. Recently, the Moskowitz laboratory reported that *Tbx5* is required in the posterior second heart field (pSHF) for atrial septation and that *Odd-skipped 1 (Osr1)* is a direct downstream target of Tbx5 in the pSHF [23].

The *Osr1* gene encodes a putative transcription factor containing four C2H2-type zinc finger motifs [24]. *Osr1* knockout mice are reported to develop AVSDs, with dilated atria and hypoplastic venous valves [25]. In the heart region, *Osr1* is expressed in the dorsal mesocardium and the atrial myocardium at E9.5. By E10.5, *Osr1* is highly expressed in the septum primum as well as in the dorsal mesocardium, and expression is maintained at least through E13.5 [23, 25]. Although it has been established that Tbx5 binds to the promoter

region of *Osr1* and regulates its transcription in the SHF [23], it still remains unclear whether and how Tbx5 and Osr1 interact in the process of atrial septation.

Methods

Mouse lines

All mouse experiments were performed with mice with a mixed B6/129/SvEv background. *Tbx5*$^{fl/+}$, *Osr1*$^{cre\text{-}ERT2/+}$ mouse lines were obtained from Dr. Ivan Moskowitz (University of Chicago). *R26R* [Gt(ROSA)26Sortm1Sor/J], *Osr1*$^{+/-}$ and *Pten*$^{fl/fl}$ mouse lines were obtained from the Jackson Laboratory. Mouse experiments were completed according to a protocol reviewed and approved by the Institutional Animal Care and Use Committee of the University of North Dakota, in compliance with the USA Public Health Service Policy on Humane Care and Use of Laboratory Animals.

Tamoxifen administration

Tamoxifen-induced activation of *CreERT2* was accomplished by oral gavage with 75 mg/kg tamoxifen (TM) at E6.5, E7.5, E9.5 or E10.5 for the genetic inducible fate mapping (GIFM) study. To induce ASDs, TM was administered at E7.5 and E8.5 or at E8.5 and E9.5 with 75 mg/kg.

Histology study

Embryos were fixed in 4% paraformaldehyde overnight at 4°C and then embedded in paraffin. Hematoxylin and eosin (HE) staining of heart sections was conducted according to standard methods to identify any defects. X-gal staining of embryos was performed as described [11]. A BrdU immunohistochemistry kit (EMD Millipore) was used for BrdU staining. For BrdU incorporation assays, 2 doses of 100 mg/kg body weight of BrdU solution (10 mg/ml) were given 3 hours and 6 hours before sacrifice at E9.0. TUNEL staining was performed by using an ApopTag plus peroxidase In-Situ apoptosis detection kit (Millipore). Rabbit anti–mouse p-Histone-H3 (ser10) (Abcam) was used for immunohistochemical staining. For colorimetric staining, slides were incubated with rabbit ImmPress reagent (Vector Labs), developed by using the DAB substrate kit (Vector Labs), and counterstained with hematoxylin.

Microdissection of pSHF and RNA extraction

E9.5 and E10.5 embryos were dissected as previously described [23, 26]. The heart, aSHF, and pSHF were collected separately in RNA Later and then stored at −20°C until genotyping was completed. Total RNA was extracted from the pSHF regions of mouse embryos hearts by using the RNeasy Mini Kit (QIAGEN), according to the manufacturer's instructions.

Quantitative RT-PCR

DNA contamination was removed from RNA samples by incubating the sample(s) with ribonuclease-free deoxyribonuclease I (RNase-free DNase I, Qiagen) at room temperature for 15 minutes. Two hundred nanograms of total RNA underwent reverse transcription by using a SuperScriptTM III Reverse Transcriptase kit (Invitrogen). qPCR was performed

with a POWER SYBER Green PCR master mix (Applied Biosystems) and an iQ5 thermal cycler (Bio-Rad) for real-time PCR. Results were analyzed by using the delta-delta Ct method with GAPDH as a normalization control [27]. Primers used are listed in Table 1.

Tbx5 Mutagenesis and Dual-Luciferase Assay

Tbx5-pcDNA 3.1 plasmid was kindly provided by the laboratory of Dr. Ivan Moskowitz (University of Chicago). Tbx5 mutants (R237Q, R237W) were made using QuikChange® XL Site-Directed Mutagenesis Kit (Agilent Technology) according to the manufacture's instruction. Primer sequences for R237Q were: 5′-CGCCAAAGGCTTT**TGG**GGCAGTGATGACC-3′ and 5′-GGTCATCACTGCC**CCA**AAAGCCTTTGGCG-3′. Primer sequences for R237Q were 5′-CGCCAAAGGCTTT**CAG**GGCAGTGATGACC-3′ and 5′-GGTCATCACTGCC**CTG**AAAGCCTTTGGCG-3′. Using FuGene HD (Promega), transient transfections were performed in HEK-293T cells. After 48 hours post-transfection, total cell lysates were prepared and luciferase activity was measured using the Dual-luciferase Reporter Assay System (Promega).

Results

Osr1 is expressed in developing DMP

Osr1 plays a role in atrial septation [25]. *Osr1* knockout mouse embryos have missing atrial septa at E11.5 [25]. To confirm this finding and to examine the possibility of a later rescue of ASD, we analyzed *Osr1* knockout embryos at E13.5 when normal atrial septation is completed. The $Osr1^{tm1RJ/+}$ mice, referred to as $Osr1^{-/+}$ mice, have a *lacZ* gene inserted into the first coding exon of the *Osr1* gene; thus, the mutation results in a functional β-galactosidase fusion gene and the loss of *Osr1* gene function [25]. We found that 50% of $Osr1^{-/-}$ embryos died before E13.5 (12/24), mostly between E11.5 and E12.5 as indicated by their tail somite numbers. $Osr1^{-/-}$ embryos that survived through E13.5 showed AVSDs, whereas no AVSDs were seen in either $Osr1^{-/+}$ or wild-type embryos (Figure 1B and 1D vs. 1A and 1C) (9/12 vs. 0/10, respectively; p=0.000367, Table 2). Our results confirm that *Osr1* is involved in atrial septation.

Previously, we reported that Osr1 is expressed in the SHF of E9.5 mouse embryos [23]; therefore, we hypothesized that *Osr1* is expressed in the developing DMP. To follow the expression of *Osr1*, we conducted X-gal staining to reveal the β-galactosidase activity in $Osr1^{-/+}$ mouse embryos at E9.5 (Figure 1E-H) and E10.5 (Figure 1I-L). β-Galactosidase was observed in the dorsal mesocardium, the DMP reflection, the PAS bud, and the atrial wall adjacent to the dorsal mesocardium at E9.5 (Figure 1E-G). At E10.5, β-galactosidase was expressed in the dorsal mesocardium, the forming DMP and PAS, and a portion of the atrial wall (Figure 1I-K). At both E9.5 and E10.5, β-galactosidase was not expressed in the ventricles, atrioventricular cushion, and outflow tract (Figure 1H and L).

Osr1-expressing cells contribute to the atrial septum progenitors between E8.0 and E11.0

To test our hypothesis that *Osr1* is required for atrial septation, we performed genetic inducible fate mapping (GIFM) [28] and thus marked descendant cells that expressed *Osr1*

during early cardiac morphogenesis. The location(s) of the marked cells was then evaluated at E13.5. Descendant cells of *Osr1*-positive cells were marked in space and time by using a tamoxifen (TM)-inducible Cre recombinase expressed from the *Osr1* locus *(Osr1cre:ERT)* [29]. Embryos were given TM (75 mg/kg) at E6.5, E7.5, E8.5, E9.5, or E10.5, and β-galactosidase expression was evaluated in $R26R^{Osr1\text{-}CreERT2/+}$ embryos at E13.5.

TM administration at E6.5 did not induce β-galactosidase expression in $R26R^{Osr1\text{-}CreERT2/+}$ embryos (data not shown). However, TM administration at E7.5, E8.5, or E9.5 resulted in β-galactosidase expression in *Osr1* descendant cells that contributed to the atrial septation and the atrial wall of $R26R^{Osr1\text{-}CreERT2/+}$ embryos (Figure 2A-C and 2E-G). The marked atrial septal structures included the whole mesenchymal core of the DMP, the PAS, and the mesenchymal cap of the PAS. However, there were very few marked cells in the atrial septum of the $R26R^{Osr1\text{-}CreERT2/+}$ embryos given TM at E10.5 (Figure 2D and 2H). We did not notice any β-galactosidase expression in the ventricular chamber and the atrioventricular cushion in all embryos; however, the free atrial wall was marked in the TM-treated $R26R^{Osr1\text{-}CreERT/+}$ embryos at all evaluated time points after E6.5 (Figure 2I-P). Considering that TM activates expression 12 hours after injection and that such lasts for 24 hours [29-31], these results suggest that *Osr1* plays a role in atrial septum progenitors between E8.0 and E11.

Regulation of *Osr1* by Tbx5 in pSHF is time-sensitive

Our previous study showed that Osr1 expression is dependent on Tbx5 transactivity in the pSHF [23]. We investigated whether Tbx5-dependent *Osr1* expression followed a time-serial change in the SHF because the proliferation of atrial progenitors is varied during different developmental stages. We dissected the pSHF, aSHF and heart as described by Moskowitz [23, 26]. In order to verify our micro-dissection, we measured the expression levels of tissue-specific genes using realtime-PCR. *Nkx2.5*, a marker for first heart field [32, 33], was strongly expressed in the E9.5 heart, but very low in aSHF and pSHF. In contrast, *Isl1* and *Tbx1*, markers for SHF [32, 33], were dominantly expressed in both aSHF and pSHF, but not in heart. The expression of *Tbx1*, a well-known transcription factor for outflow tract development [32, 34-36], was significantly higher in aSHF than in pSHF. In addition, *Tbx5* and *Osr1* expression was remarkably high in pSHF and extremely low in aSHF, which is in consistent with previous reports [23, 25]. These results verified our micro-dissection on heart, pSHF and aSHF.

Osr1 expression in the dorsal mesocardium of $Tbx5^{+/-}$ and wild-type mouse embryos was measured by RT-PCR at E8.5, E9.5, and E10.5. Knockout of one copy of *Tbx5* caused diminished *Osr1* expression at E8.5 (0.669 ± 0.087, p=0.0001) and E9.5 (0.544 ± 0.105, p=0.006) but not at E10.5 (0.986 ± 0.065, p=0.837) (Figure 3B). However, expression of *Isl1* was unchanged in $Tbx5^{+/-}$ embryos at both E8.5 (1.146 ± 0.117) and E9.5 (0.908 ± 0.104).

Osr1 interacts with *Tbx5* in atrial septum progenitors

We hypothesized that *Osr1* interacts with *Tbx5* for atrial septation. We tested this hypothesis by analyzing embryos with compound haploinsufficiency for *Osr1* and *Tbx5* ($Osr1^{+/-}$;

Tbx5$^{+/-}$). *Osr1*$^{+/-}$ embryos did not show ASDs (0/8; Figure 3C and 3F), and 40% of E13.5 *Tbx5*$^{+/-}$ mouse embryos developed AVSDs, as reported earlier [23, 25, 37] (Figure 3D and 3G). The incidence of AVSDs was significantly greater in *Osr1*$^{+/-}$*; Tbx5*$^{+/-}$ mouse embryos (11/11, Figure 3E and 3H) than in either *Osr1*$^{+/-}$ embryos (0/8, p=0.001) or *Tbx5*$^{+/-}$- embryos (5/10, p=0.0149, Table 2).

We showed that *Osr1*-expressing cells contributed to atrial septum progenitors between E8.0 and E11. Therefore, we tested our hypothesis that *Tbx5* interacts with *Osr1* by analyzing *Osr1* and *Tbx5*-conditional haploinsufficiency, using *Osr1:CreERT2*. The *Osr1:CreERT2* is a "knock-in" allele that both abolishes *Osr1* gene function and encodes TM-inducible Cre recombinase (CreERT2). The conditional knockdown of *Tbx5* in *Osr1*-expressing cells that constituted atrial septum progenitors (*Tbx5*$^{Osr1\text{-}CreERT2/+}$) was activated by TM administration at E7.5 and E8.5 or at E8.5 and E9.5. The *Tbx5*$^{Osr1\text{-}CreERT2/+}$ embryos had one copy of conditionally abolished *Tbx5* combined with *Osr1* abolishment. We observed AVSDs in 63.7% of *Tbx5*$^{Osr1\text{-}CreERT2/+}$ embryos at E13.5 (TM at E7.5 and 8.5) (Figure 3K and 3N, 7/11), whereas AVSDs were absent in *Osr1*$^{CreERT2/+}$ embryos (0/7, p=0.0035; Figure 3J and 3M) and *Tbx5*$^{fl/+}$ embryos (0/7, p=0.0035; Figure 3I and 3L, Table 2). For those embryos treated with TM at E8.5 and E9.5, the incidence of AVSDs was similar to that of embryos treated with TM at E7.5 and E8.5 (Table 2). These results suggest that *Tbx5* genetically interacts with *Osr1* in atrial septum progenitors.

Tbx5 and *Osr1* interact in regulating the proliferation of pSHF cardiac progenitors

Increased apoptosis of pSHF cardiac progenitors could lead to the absence of the atrial septum. Indeed, increased nephrogenic mesenchymal cell death has been observed in *Osr1* knockout mouse embryos [25]. Therefore, we assessed cell survival in *Osr1*$^{-/-}$ embryos at E10.5. TUNEL staining did not detect apoptotic cells in the pSHF and the DMP region of either *Osr1*$^{-/-}$ or wild-type embryos (Figure 4A-D); this absence of apoptotic cells suggests that Osr1 is not involved in cell survival in this region.

Although neither Tbx5 nor Osr1 plays a role in the survival of pSHF cardiac progenitors [23], we could not exclude the possibility that Tbx5 interacts or co-operates with Osr1 in regulating cell survival. However, results of the TUNEL assays showed that no apoptotic cells were present within the pSHF and the DMP in *Tbx5*$^{Osr1\text{-}CreERT2/+}$ and littermate control embryos (Figure 4E-H).

Because Tbx5 is required for proliferation of atrial progenitors (Xie et al., 2012), we hypothesized that Osr1 also regulates cell proliferation in the pSHF. Using BrdU incorporation assay, we determined the proportion of proliferating cells in the pSHF of *Osr1*$^{-/-}$ and wild-type embryos at E9.5. By counting a total of 500 cells in the pSHF region of five serial sections across the DMP reflection from four embryos (Figure 4J-L, framed region), we found that *Osr1*$^{-/-}$ embryos had 54.8% fewer BrdU-positive cells than did wild-type embryos (Figure 4K, L, and I, J; 31.7% ± 2.52% vs. 70.0% ± 4.58%, respectively; p=0.008). These results suggest that *Osr1* is required for the proliferation of pSHF cardiac progenitors.

Because both *Tbx5* and *Osr1* are required in the proliferation of pSHF atrial progenitors, we tested the hypothesis that *Tbx5* and *Osr1* interact in regulating cell proliferation in the pSHF. Using BrdU incorporation assays, we notice a substantial decrease in the number of proliferating cells in the SHF of $Tbx5^{Osr1\text{-}CreERT2/+}$ embryos at E10.5, a result in contrast to that seen in either $Osr1^{CreERT2/+}$ *or* $Tbx5^{fl/+}$ embryos (Figure 4N vs. P). The number of proliferating cells in the pSHF around and in the DMP of $Tbx5^{Osr1\text{-}CreERT2/+}$ embryos was 36.5% less than that in$Osr1^{CreERT2/+}$ embryos (Figure 4R, 48.7% ± 3.06% vs. 76.7% ± 5.03%, respectively; p=0.001). In contrast, the BrdU-positive cells in the first bronchial arch did not differ between $Tbx5^{Osr1\text{-}CreERT2/+}$ *embryos* and $Osr1^{CreERT2/+}$ embryos (Figure 4M vs 4O, 82% ± 2.65% vs. 81.7% ± 2.52%, respectively; p=0.882). These results demonstrate that *Tbx5* and *Osr1* interact in regulating pSHF cell proliferation but not in cell survival.

Tbx5 and *Osr1* interact in regulating the cell cycle progression of pSHF cardiac progenitors

We tested the hypothesis that *Osr1* regulates pSHF cell cycle progression by conducting phosphorylated Ser10-H3-histone (H3S10) immunohistochemical analysis, which differentially marks mitotic cells in G2 (staining is punctate) and M phases (staining is homogeneous) [23, 38]. Evaluation of 500 cells in the pSHF around and in the DMP (Figure 5C and D, framed region) found that the number of H3S10-positive cells in the M phase of $Osr1^{-/-}$ embryos was 53.7% less than that in wild-type embryos (Figure 5I, red bar, 10.3% ± 0.58% vs. 26.7% ± 0.57%, respectively; p=0.002). However, there was no difference in the proportion of G2 cells in pSHF (Figure 5I, blue bar, 22.3% ± 0.58% vs. 23.0 % ± 1.00 %, respectively; p=0.18). Therefore, *Osr1* is required for progression of pSHF cells through the M phase of the cell cycle.

Osr1 expression in the pSHF is under the transcriptional control of Tbx5 [23], and Tbx5 and Osr1 genetically interact in atrial septation (this study). We hypothesized that the interaction of *Tbx5* and *Osr1* in SHF is required for cell cycle progression. As shown in Figure 5 (H and G), the number of mitotic pSHF progenitors, which were marked by H3S10, in the $Tbx5^{Osr1\text{-}CreERT2/+}$ embryos was 26.6% less than the number in $Osr1^{CreERT2/+}$ embryos. In addition, the number of pSHF progenitors in the G2 phase in $Tbx5^{Osr1\text{-}CreERT2/+}$ embryos was 24.3% less than that in the $Osr1^{CreERT2/+}$ embryos at E10.5 (Figure 5J, 7.01% ± 0.62% vs. 9.55% ± 0.56%, respectively; p=0.006 for the M phase; 10.9% ± 0.32% vs.14.4% ± 0.92%, respectively; p=0.003 for the G2 phase). We have shown that pSHF cells of either $Osr1^{-/-}$ (Figure 5I) or $Tbx5^{+/-}$ embryos have defects only in the M phase [23]. The more severe cell cycle defects of $Tbx5^{Osr1\text{-}CreERT2/+}$ pSHF cardiac progenitors suggest an interactive role of *Tbx5* and *Osr1* in cell cycle regulation.

We examined the expression level of several cell cycle genes, including *Cdk4*, *Cdk6*, *Cyclin D2*, *Cdkn1a*, *Trp53* and *Pten*, that are responsible for the G1-S phase transition in pSHF of wild-type, $Tbx5^{+/-}$, $Osr1^{+/-}$, and $Tbx5^{+/-};Osr1^{+/-}$ embryos at E9.5. The expression of *Cdk6* and *Cyclin D2* was significantly less in pSHF tissues of $Tbx5^{+/-}$, $Osr1^{+/-}$, and $Tbx5^{+/-};Osr1^{+/-}$ mouse embryos than in those of wild-type embryos (Figure 5K). Specifically, there was a further reduction of *Cdk6* expression in $Tbx5^{+/-};Osr1^{+/-}$ pSHF as compared with that in $Tbx5^{+/-}$ pSHF (0.020 ± 0.009 vs. 0.448 ± 0.079, respectively;

p=0.0001) or *Osr1*$^{+/-}$ pSHF (0.020 ± 0.009 vs.0.446 ± 0.058, respectively; p=0.006) (Figure 5K).

These results suggest that Tbx5 and Osr1 interact at the cellular and molecular level in regulating the cell cycle progression of cardiac progenitors in the pSHF.

Genetically targeted disruption of *Pten* expression in atrial septum progenitors rescued ASDs in *Tbx5*$^{Osr1\text{-}CreERT2/+}$ embryos

Phosphatase and tensin homolog (*Pten*) is a tumor suppressor that negatively regulates cell cycle progression by negatively regulating the PI-3K/AKT pathway and Cyclin D expression; thus, *Pten* inhibits cell proliferation and induces G1-S phase arrest [39-44]. We hypothesized that disruption of *Pten* in atrial septum progenitors will rescue ASDs in *Tbx5*$^{Osr1\text{-}CreERT2/+}$ embryos because decreased *Pten* expression will release G1-S phase arrest and this release will lead to progression through the cell cycle. In control *Pten* $^{Osr1\text{-}CreERT2/+}$ embryos, normal atrial septal development was observed at E14.5 (7/7, Figure 5M and 5P). Conditionally repressing *Pten* expression in atrial septum progenitors by *Osr1:CreERT2* resulted in the rescue of AVSDs in *Tbx5*$^{Osr1\text{-}CreERT2/+}$ embryos: AVSDs were observed in 16.7% of *Tbx5*$^{Osr1\text{-}CreERT2/+}$*; PTEN* $^{Osr1\text{-}CreERT2/+}$ embryos (1/6) in contrast to 66.7% of *Tbx5*$^{Osr1\text{-}CreERT2/+}$ embryos (8/12, p=0.0062) (Table 2, Figure 5Q vs. 5O).

To test the hypothesis that *Pten* knockdown in the pSHF normalizes the cell cycle defect, we quantitated the percentage of pSHF cells at E9.5 in G2 phase and M phase by H3S10 staining. The results showed no significant increase of G2 and M phase, marked by H3S10 positive, in pSHF of *PTEN*$^{Osr1\text{-}CreERT2/+,}$ comparing to *Tbx5*$^{fl/+}$*;Pten*$^{fl/+}$ embryos (Figure 5R, G2: 13.17% ±0.8% vs 12.36% ±1.2%.; M: 8.95% ± 1.01% vs.8.41% ±1.66%, p=0.81). However, there was rescue of decreased G2 and M phase in pSHF of *Tbx5*$^{Osr1/+}$, when one copy of *Pten* gene was knockout in pSHF (Figure 5R, G2: 8.1% ±1.37% vs. 11.47% ±1.72%; M: 5.83% ± 1.62% vs.9.38% ±0.96%, p=0.037) and the number of H3S10 positive cells in pSHF of *PTEN*$^{Osr1\text{-}CreERT2/+,}$ *Tbx5*$^{Osr1\text{-}CreERT2/+,}$ was not different than that of *PTEN*$^{fl/+,}$ *Tbx5*$^{fl/+}$ (Figure 5R, G2: 11.47% ±1.72% vs. 12.36% ±1.2%; M: 9.38% ±0.96% vs. 8.41% ±1.66%, p=0.79). These results suggest that deletion of *Pten* rescues the morphologic defects in *Tbx5*$^{Osr1\text{-}CreERT2/+}$ embryos by a mechanism that includes normalization of cell cycle progression.

Integrity of the Hedgehog (Hh) signaling pathway was differentially regulated at E9.5 and E10.5

Previous work demonstrated that Tbx5 acts upstream and parallel to Hh signaling in the SHF and that *Osr1* is a target downstream gene required for atrial septation [23]; however, the detailed interaction among Tbx5, Osr1, and Hh signaling is unclear. We quantitatively evaluated the expression of *Smo*, *Gli1*, and *Gli3* genes, which are key modulators of Hh signaling pathway, in the pSHF of *Osr1*$^{-/-}$ embryos at E9.5. *Smo* expression was decreased in *Osr1*$^{-/-}$ embryos (0.314 ± 0.104, p=0.010), but Gli1 expression (0.924 ± 0.517, p=0.788) and *Gli3* expression (1.172 ± 0.238, p=0.329) was not (Figure 6A). As previously reported,

Tbx5 expression was not changed in *Osr1* knockout mouse embryos (1.493 ± 0.521, p=0.213) [25].

We hypothesized that Tbx5 and Osr1 interactively regulate Hedgehog (Hh) signaling, and we tested this hypothesis by quantitatively evaluating the expression of *Smo*, *Gli1*, and *Gli3* in the pSHF of *Tbx5*$^{+/-}$, *Osr1*$^{+/-}$, *Tbx5*$^{+/-}$;*Osr1*$^{+/-}$, and wild-type mouse embryos, at both E9.5 and E10.5 (Figure 6B and 6C). Real-time PCR analysis indicated that *Smo* and *Gli1* expression was significantly reduced at E9.5 in the pSHF of *Tbx5*$^{+/-}$ embryos (*Smo*: 0.570 ± 0.099, p=0.007; *Gli1*: 0.408 ± 0.125, p=0.002) and *Tbx5*$^{+/-}$;*Osr1*$^{+/-}$ embryos (*Smo*: 0.521 ± 0.108, p=0.021; *Gli1*: 0.275 ± 0.080, p=0.001) but not *Osr1*$^{+/-}$ embryos (*Smo:* 1.142 ± 0.141, p=0.296; *Gli1*: 1.000 ± 0.503, p=0.997). However, *Smo* and *Gli1* expression were not changed in the pSHF of *Tbx5*$^{+/-}$ embryos (*Smo*: 1.149 ± 0.250, p=0.171; *Gli1*: 1.243 ± 0.177, p=0.141), *Osr1*$^{+/-}$ embryos (*Smo:* 1.137 ± 0.223, p=0.453; *Gli1*: 1.056 ± 0.145, p=0.699), or *Tbx5*$^{+/-}$;*Osr1*$^{+/-}$ embryos (*Smo:* 1.099 ± 0.230, p=0.587; *Gli1*: 1.116 ± 0.065, p=0.302) at E10.5. At E9.5, expression levels of other tested genes—*Foxf1a, Fgf8, Fgf15, Myl2, Myl3, Myl7,* and *Myl9*— were similar to those at E10.5. None of these genes showed expression change in *Osr1*$^{+/-}$ embryos at both E9.5 and E10.5.

Osr1 transcription is affected by *Tbx5* mutation that causes Holt-Oram Syndrome (HOS)

It has been estimated that 74% of patients who meet strict diagnostic criteria for Holt-Oram Syndrome (HOS) will have an identifiable mutation in the *TBX5* gene [45]. The mutation spectrum in the *TBX5* gene is wide. So far, more than 30 reported single base pair substitutions have been reported to result HOS, including R237W and R237Q that are among the top five most reported mutations responsible for about 50% of cases of HOS [46]. We hypothesized that disrupted *Osr1* trans-activation induced by *TBX5* mutation was a potential cause of ASD in HOS. We replicated the point mutation R237Q and R237W of human *TBX5* in mouse and generated mutated mouse Tbx5 accordingly (see Methods). Previously, two distinct *Osr1* genomic regions, Osr1F1 and Osr1F4, responsive to Tbx5 trans-activation have been reported [23]. Our results show that R237Q-Tbx5 and R237W-Tbx5 are unable to induce trans-activated *luciferase* expression from Osr1F1 and Osr1F4, while *widltype* Tbx5 did (Figure 7A).

The crystal structures of human TBX5 T-box domain have been demonstrated both in its DNA-free form and DNA-bound form [47]. In light of this development, we investigated if and how the point mutation (R237Q-Tbx5 and R237W-Tbx5) affected the DNA binding ability of Tbx5. We first generated the structures of those two mutants using Rosetta software designed for protein structure modeling [48]. ΔΔG value given by the difference in rosetta energy between the wild-type structure and the point mutant structure is used to predict the change in protein stability. For R237W-Tbx5 and R237Q-Tbx5, the ΔΔG value is 0.941 and 3.267 respectively, suggesting that both these mutants can destabilize the protein. We further analyzed how the binding structure of mutant Tbx5 and DNA was changed using Pymol (version 1.7), which is designed for molecular visualization. We especially studied a region including the 3_{10}-helix at the C-terminus of the T-box domain (residues F232-R237) which is inserted into the minor groove of DNA in binding form. We predicted that the hydrogen bonds (H-bond) between Lys234 and DNA that usually maintain the binding

structure of DNA and wildtype *Tbx5* are missing in both the two mutants, together with several interactions within this region (Figure 7B). Specifically, the salt bridge between Arg237 and Glu228 no longer existed in R237W-Tbx5, as well as the H-bond between Arg237 and Asn230. In R237Q-Tbx5, instead of forming H-bond between Arg237 and Asn230, a new H-bond formed between Arg237 and Lys234. These results suggest that mutation R237W and R237Q can destabilize Tbx5 and induce conformational changes within the 3_{10}-helix region, thus reducing its ability to bind to promoter region of Osr1.

Discussion

In the present study, we demonstrated that *Osr1*-expressing cells contribute to atrial septum progenitors between E8.0 and E10.5, a time during which Hh signaling is required for the specification of atrial septal progenitors (Figures 1 and 2) [11]. *Osr1* expression in the pSHF was dependent on the level of Tbx5 at E8.5 and E9.5 but not at E10.5 (Figure 3A); this result suggests that the embryo stage before E10.5 is critical for the interaction of Tbx5 with Osr1 in atrial septation. Significantly more AVSDs (primum ASD) occurred in embryos with compound haploinsufficiency for *Tbx5* and *Osr1* than in those with single haploinsufficiency for *Tbx5* or *Osr1* (Figure 3 and Table 2). The increased incidence of AVSD in mice with compound haploinsufficiency for *Tbx5* and *Osr1* was associated with a severe proliferation defect in atrial progenitors through defective cell cycle progression and was related at least in part with decreased *CdK6* regulation (Figures 4 and 5). Remarkably, genetically targeted disruption of *Pten* expression in atrial septum progenitors rescued AVSDs caused by *Tbx5* and *Osr1* compound haploinsufficiency via rescue of cell proliferation in pSHF (Figure 5). A significant reduction in *Smo* expression was observed in the pSHF of *Osr1* knockout embryos at E9.5, implying a role for Osr1 in regulating Hh signaling (Figure 6). Furthermore, Osr1 transcription was blocked by Tbx5 mutation by luciferase reporter assay (Figure 7), which suggests that disrupted interaction between tbx5 and Osr1 is a potential mechanism in Holt-Oram Syndrome (HOS).

Wang et al. reported the occurrence of ASDs in *Osr1* knockout mouse embryos at E11.5 [25], a result that suggested a role for Osr1 in atrial septation. However, it remained unclear when and where Osr1 is required for atrial septation; therefore, this topic was a focus of our study. We showed that Osr1 was expressed in the dorsal mesocardium, the forming DMP, and the PAS, but not in the ventricles, atrioventricular cushion, and outflow tract at E9.5 and E10.5 (Figure 1) [23]. Using GIFM, we found that Osr1 descendant cells contributed to the PAS and DMP from E8 to E10.5 (Figure 2), which overlaps where and when atrial septal progenitors, marked by Gli1Cre positive [10, 11, 23], are required by atrial septation. We conclude that Osr1 is required in the atrial septal progenitors from E8 to E10.5.

The implication of *Tbx5* and *Osr1* interaction in the SHF for atrioventricular septation buttresses our previous implication of *Tbx5* and a growing body of literature indicating that SHF defects can cause AVSDs [10, 11, 23, 49-51]. In the present report, we showed an increased incidence of primum AVSDs in *Tbx5* and *Osr1* compound heterozygotes (Figure 3), a result that confirmed the interaction between Tbx5 and Osr1 in the pSHF for atrial septation. The fact that mutation of Tbx5 found in human blocked the transactivation of Osr1 (Figure 7A) also suggested that disruption of Tbx5 and Osr1 interaction as a potential

molecular mechanism of HOS. We observed that the numbers of cells in the G2 and M phases were decreased in the pSHF of *Tbx5* and *Osr1* compound heterozygotes. Expression of *Cdk6*, which is required for G1-S phase progression and is a direct transcription target of Tbx5 [23], was shown to depend on *Tbx5-Osr1* interaction in the pSHF (Figure 5). In addition, a specific decrement in expression of *Pten*, a tumor repressor that negatively regulates the *Cyclin D* gene, rescued the cardiac morphogenesis defects caused by *Tbx5* and *Osr1* double haploinsufficiency via repair of cell cycle defects (Figure 5). These observations support the concept that *Tbx5* and *Osr1* interact to promote SHF cardiac progenitor proliferation, promote expression of cell cycle genes related to the G1-S phase transition, and generate a progenitor pool capable of supporting atrial septum morphogenesis (Figure 7C).

Interestingly, we were not able to detect significant differences in *Osr1* expression in the pSHF of $Tbx5^{+/-}$; $Osr1^{+/-}$ embryos and of $Tbx5^{+/-}$ embryos at all embryonic stages tested (Figure 6B vs. C); however, all $Tbx5^{+/-}$; $Osr1^{+/-}$ embryos displayed ASDs, whereas only 40% of *Tbx5* single heterozygotes had AVSDs. It is possible that enlarging the sample size may disclose the trivial but critical dose difference of *Osr1* in the pSHF of $Tbx5^{+/-}$; $Osr1^{+/-}$ embryos and $Tbx5^{+/-}$ embryos. Possible evidence is that the level of *Cdk6* in the pSHF was significantly lower in $Tbx5^{+/-}$; $Osr1^{+/-}$ embryos than in $Tbx5^{+/-}$ or $Osr1^{+/-}$ embryos (Figure 5K). In addition, both our realtime PCR results (Figure 2A) and RNA sequencing data (data not shown) showed a trend of a 20% reduction in *Osr1* expression in the pSHF of $Tbx5^{+/-}$; $Osr1^{+/-}$ embryos as compared with that in $Tbx5^{+/-}$ embryos at E9.5. In addition, the greater incidence of ASD in $Tbx5^{+/-}$; $Osr1^{+/-}$ embryos might be associated with the level of *Osr1* expression that was 65% of that in wild-type throughout all developmental stages, but the level of *Osr1* expression was normal at E10.5 in the pSHF of $Tbx5^{+/-}$ mouse embryos.

The finding that Tbx5 directly regulates *Osr1* transcription in the pSHF only before E10.5 suggests that *Osr1* activity, which is under Tbx5 regulation in the pSHF, is strictly embryonic stage-dependent. In addition, the finding implies that different molecular signaling in the pSHF is required before and after E10.5. It is noted that not only *Osr1* but also the integrity of Hh signaling of $Tbx5^{+/-}$ mouse embryos was affected at E9.5 but not at E10.5. These results extend our understanding and provide evidence to demonstrate that the signaling networks in the pSHF are not only spatially but also temporally regulated. Before E10.5, *Tbx5* directly transactivates *Osr1* and interactively regulates *Hh* signaling and expression of genes involved in cell cycle regulation (Figure 7C). At E10.5, *Osr1* transcription and Hh signaling in the pSHF are no longer directly dependent on level of *Tbx5*. Detailed roles for the requirement of these important cardiac transcription factors in atrial septation and human ASDs at later developmental stages, such as after E10.5, should be further studied.

Acknowledgments

This project was supported by grants from the National Institutes of Health (NIH-1R15HL117238 to LX and National Center for Research Resources, 5P20RR016471-12/8 P20 GM103442-12 to LX and KZ) and the American Heart Association (Scientist Development Grant to LX).

References

1. Kaplan S. Congenital heart disease in adolescents and adults. Natural and postoperative history across age groups. Cardiol Clin. 1993; 11:543–56. [PubMed: 8252558]
2. Malumbres M, Barbacid M. Mammalian cyclin-dependent kinases. Trends Biochem Sci. 2005; 30:630–41. [PubMed: 16236519]
3. Snarr BS, Kern CB, Wessels A. Origin and fate of cardiac mesenchyme. Developmental dynamics : an official publication of the American Association of Anatomists. 2008; 237:2804–19. [PubMed: 18816864]
4. Webb S, Brown NA, Anderson RH. Formation of the atrioventricular septal structures in the normal mouse. Circulation research. 1998; 82:645–56. [PubMed: 9546373]
5. Zhang XM, Ramalho-Santos M, McMahon AP. Smoothened mutants reveal redundant roles for Shh and Ihh signaling including regulation of L/R asymmetry by the mouse node. Cell. 2001; 105:781–92. [PubMed: 11440720]
6. Lan Y, Liu H, Ovitt CE, Jiang R. Generation of Osr1 conditional mutant mice. Genesis. 2011; 49:419–22. [PubMed: 21462293]
7. Wessels A, Anderson RH, Markwald RR, Webb S, Brown NA, Viragh S, et al. Atrial development in the human heart: an immunohistochemical study with emphasis on the role of mesenchymal tissues. The Anatomical record. 2000; 259:288–300. [PubMed: 10861362]
8. Anderson RH, Webb S, Brown NA, Lamers W, Moorman A. Development of the heart: (2) Septation of the atriums and ventricles. Heart. 2003; 89:949–58. [PubMed: 12860885]
9. Galli D, Dominguez JN, Zaffran S, Munk A, Brown NA, Buckingham ME. Atrial myocardium derives from the posterior region of the second heart field, which acquires left-right identity as Pitx2c is expressed. Development. 2008; 135:1157–67. [PubMed: 18272591]
10. Goddeeris MM, Rho S, Petiet A, Davenport CL, Johnson GA, Meyers EN, et al. Intracardiac septation requires hedgehog-dependent cellular contributions from outside the heart. Development. 2008; 135:1887–95. [PubMed: 18441277]
11. Hoffmann AD, Peterson MA, Friedland-Little JM, Anderson SA, Moskowitz IP. sonic hedgehog is required in pulmonary endoderm for atrial septation. Development. 2009; 136:1761–70. [PubMed: 19369393]
12. Mommersteeg MT, Soufan AT, de Lange FJ, van den Hoff MJ, Anderson RH, Christoffels VM, et al. Two distinct pools of mesenchyme contribute to the development of the atrial septum. Circulation research. 2006; 99:351–3. [PubMed: 16873717]
13. Snarr BS, O'Neal JL, Chintalapudi MR, Wirrig EE, Phelps AL, Kubalak SW, et al. Isl1 expression at the venous pole identifies a novel role for the second heart field in cardiac development. Circulation research. 2007; 101:971–4. [PubMed: 17947796]
14. Tian Y, Cohen ED, Morrisey EE. The importance of Wnt signaling in cardiovascular development. Pediatric cardiology. 2010; 31:342–8. [PubMed: 19967349]
15. Basson CT, Bachinsky DR, Lin RC, Levi T, Elkins JA, Soults J, et al. Mutations in human TBX5 [corrected] cause limb and cardiac malformation in Holt-Oram syndrome. Nat Genet. 1997; 15:30–5. [PubMed: 8988165]
16. Garg V, Kathiriya IS, Barnes R, Schluterman MK, King IN, Butler CA, et al. GATA4 mutations cause human congenital heart defects and reveal an interaction with TBX5. Nature. 2003; 424:443–7. [PubMed: 12845333]
17. Li QY, Newbury-Ecob RA, Terrett JA, Wilson DI, Curtis AR, Yi CH, et al. Holt-Oram syndrome is caused by mutations in TBX5, a member of the Brachyury (T) gene family. Nat Genet. 1997; 15:21–9. [PubMed: 8988164]
18. Schott JJ, Benson DW, Basson CT, Pease W, Silberbach GM, Moak JP, et al. Congenital heart disease caused by mutations in the transcription factor NKX2-5. Science. 1998; 281:108–11. [PubMed: 9651244]
19. Bruneau BG, Logan M, Davis N, Levi T, Tabin CJ, Seidman JG, et al. Chamber-specific cardiac expression of Tbx5 and heart defects in Holt-Oram syndrome. Developmental biology. 1999; 211:100–8. [PubMed: 10373308]

20. Hiroi Y, Kudoh S, Monzen K, Ikeda Y, Yazaki Y, Nagai R, et al. Tbx5 associates with Nkx2-5 and synergistically promotes cardiomyocyte differentiation. Nat Genet. 2001; 28:276–80. [PubMed: 11431700]
21. Bruneau BG. The developing heart and congenital heart defects: a make or break situation. Clinical genetics. 2003; 63:252–61. [PubMed: 12702154]
22. Mori AD, Zhu Y, Vahora I, Nieman B, Koshiba-Takeuchi K, Davidson L, et al. Tbx5-dependent rheostatic control of cardiac gene expression and morphogenesis. Developmental biology. 2006; 297:566–86. [PubMed: 16870172]
23. Xie L, Hoffmann AD, Burnicka-Turek O, Friedland-Little JM, Zhang K, Moskowitz IP. Tbx5-hedgehog molecular networks are essential in the second heart field for atrial septation. Dev Cell. 2012; 23:280–91. [PubMed: 22898775]
24. Coulter DE, Swaykus EA, Beran-Koehn MA, Goldberg D, Wieschaus E, Schedl P. Molecular analysis of odd-skipped, a zinc finger encoding segmentation gene with a novel pair-rule expression pattern. The EMBO journal. 1990; 9:3795–804. [PubMed: 2120051]
25. Wang Q, Lan Y, Cho ES, Maltby KM, Jiang R. Odd-skipped related 1 (Odd 1) is an essential regulator of heart and urogenital development. Developmental biology. 2005; 288:582–94. [PubMed: 16223478]
26. Hoffmann AD, Yang XH, Burnicka-Turek O, Bosman JD, Ren X, Steimle JD, et al. Foxf genes integrate tbx5 and hedgehog pathways in the second heart field for cardiac septation. PLoS Genet. 2014; 10:e1004604. [PubMed: 25356765]
27. Schmittgen TD, Livak KJ. Analyzing real-time PCR data by the comparative C(T) method. Nat Protoc. 2008; 3:1101–8. [PubMed: 18546601]
28. Joyner AL, Zervas M. Genetic inducible fate mapping in mouse: establishing genetic lineages and defining genetic neuroanatomy in the nervous system. Developmental dynamics : an official publication of the American Association of Anatomists. 2006; 235:2376–85. [PubMed: 16871622]
29. Mugford JW, Sipila P, McMahon JA, McMahon AP. Osr1 expression demarcates a multi-potent population of intermediate mesoderm that undergoes progressive restriction to an Osr1-dependent nephron progenitor compartment within the mammalian kidney. Dev Biol. 2008; 324:88–98. [PubMed: 18835385]
30. Hu YC, Okumura LM, Page DC. Gata4 is required for formation of the genital ridge in mice. PLoS Genet. 2013; 9:e1003629. [PubMed: 23874227]
31. Mugford JW, Sipila P, Kobayashi A, Behringer RR, McMahon AP. Hoxd11 specifies a program of metanephric kidney development within the intermediate mesoderm of the mouse embryo. Dev Biol. 2008; 319:396–405. [PubMed: 18485340]
32. Watanabe Y, Zaffran S, Kuroiwa A, Higuchi H, Ogura T, Harvey RP, et al. Fibroblast growth factor 10 gene regulation in the second heart field by Tbx1, Nkx2-5, and Islet1 reveals a genetic switch for down-regulation in the myocardium. Proc Natl Acad Sci U S A. 2012; 109:18273–80. [PubMed: 23093675]
33. Kelly RG. The second heart field. Curr Top Dev Biol. 2012; 100:33–65. [PubMed: 22449840]
34. Zhang Z, Cerrato F, Xu H, Vitelli F, Morishima M, Vincentz J, et al. Tbx1 expression in pharyngeal epithelia is necessary for pharyngeal arch artery development. Development. 2005; 132:5307–15. [PubMed: 16284121]
35. Rana MS, Theveniau-Ruissy M, De Bono C, Mesbah K, Francou A, Rammah M, et al. Tbx1 coordinates addition of posterior second heart field progenitor cells to the arterial and venous poles of the heart. Circ Res. 2014; 115:790–9. [PubMed: 25190705]
36. Liao J, Aggarwal VS, Nowotschin S, Bondarev A, Lipner S, Morrow BE. Identification of downstream genetic pathways of Tbx1 in the second heart field. Developmental biology. 2008; 316:524–37. [PubMed: 18328475]
37. Bruneau BG, Nemer G, Schmitt JP, Charron F, Robitaille L, Caron S, et al. A murine model of Holt-Oram syndrome defines roles of the T-box transcription factor Tbx5 in cardiogenesis and disease. Cell. 2001; 106:709–21. [PubMed: 11572777]
38. Crosio C, Fimia GM, Loury R, Kimura M, Okano Y, Zhou H, et al. Mitotic phosphorylation of histone H3: spatio-temporal regulation by mammalian Aurora kinases. Mol Cell Biol. 2002; 22:874–85. [PubMed: 11784863]

39. Songyang Z, Baltimore D, Cantley LC, Kaplan DR, Franke TF. Interleukin 3-dependent survival by the Akt protein kinase. Proc Natl Acad Sci U S A. 1997; 94:11345–50. [PubMed: 9326612]
40. Stambolic V, Suzuki A, de la Pompa JL, Brothers GM, Mirtsos C, Sasaki T, et al. Negative regulation of PKB/Akt-dependent cell survival by the tumor suppressor PTEN. Cell. 1998; 95:29–39. [PubMed: 9778245]
41. Di Cristofano A, Pandolfi PP. The multiple roles of PTEN in tumor suppression. Cell. 2000; 100:387–90. [PubMed: 10693755]
42. Diao L, Chen YG. PTEN, a general negative regulator of cyclin D expression. Cell Res. 2007; 17:291–2. [PubMed: 17426697]
43. Huang W, Chang HY, Fei T, Wu H, Chen YG. GSK3 beta mediates suppression of cyclin D2 expression by tumor suppressor PTEN. Oncogene. 2007; 26:2471–82. [PubMed: 17043650]
44. Ramaswamy S, Nakamura N, Vazquez F, Batt DB, Perera S, Roberts TM, et al. Regulation of G1 progression by the PTEN tumor suppressor protein is linked to inhibition of the phosphatidylinositol 3-kinase/Akt pathway. Proc Natl Acad Sci U S A. 1999; 96:2110–5. [PubMed: 10051603]
45. McDermott DA, Bressan MC, He J, Lee JS, Aftimos S, Brueckner M, et al. TBX5 genetic testing validates strict clinical criteria for Holt-Oram syndrome. Pediatr Res. 2005; 58:981–6. [PubMed: 16183809]
46. Heinritz W, Shou L, Moschik A, Froster UG. The human TBX5 gene mutation database. Hum Mutat. 2005; 26:397. [PubMed: 16134140]
47. Stirnimann CU, Ptchelkine D, Grimm C, Muller CW. Structural basis of TBX5-DNA recognition: the T-box domain in its DNA-bound and -unbound form. J Mol Biol. 2010; 400:71–81. [PubMed: 20450920]
48. Smith CA, Kortemme T. Backrub-like backbone simulation recapitulates natural protein conformational variability and improves mutant side-chain prediction. J Mol Biol. 2008; 380:742–56. [PubMed: 18547585]
49. Briggs LE, Kakarla J, Wessels A. The pathogenesis of atrial and atrioventricular septal defects with special emphasis on the role of the dorsal mesenchymal protrusion. Differentiation. 2012; 84:117–30. [PubMed: 22709652]
50. Briggs LE, Phelps AL, Brown E, Kakarla J, Anderson RH, van den Hoff MJ, et al. Expression of the BMP receptor Alk3 in the second heart field is essential for development of the dorsal mesenchymal protrusion and atrioventricular septation. Circ Res. 2013; 112:1420–32. [PubMed: 23584254]
51. Tian Y, Yuan L, Goss AM, Wang T, Yang J, Lepore JJ, et al. Characterization and in vivo pharmacological rescue of a Wnt2-Gata6 pathway required for cardiac inflow tract development. Dev Cell. 2010; 18:275–87. [PubMed: 20159597]

Abbreviations

AVSDs	atrioventricular septal defects
ASDs	atrial septal defects
SV	spina vestobuli
DMP	dorsal mesenchymal protrusion
PAS	primary atrial septum
SHF	second heart field
HOS	Holt-Oram syndrome
Osr1	Odd-skipped 1

Highlights

1. *Osr1* and *Tbx5* interact for cardiac septation
2. Regulation of Osr1 by Tbx5 in posterior SHF is time-sensitive.
3. *Tbx5* and *Osr1* interact to regulate the atrial progenitor cell cycle progression.
4. *Pten* knockdown rescued AVSDs caused by *Osr1* and *Tbx5* compound haploinsufficiency.
5. Integrity of the Hh signaling was dependent on Osr1 level and is time-sensitive

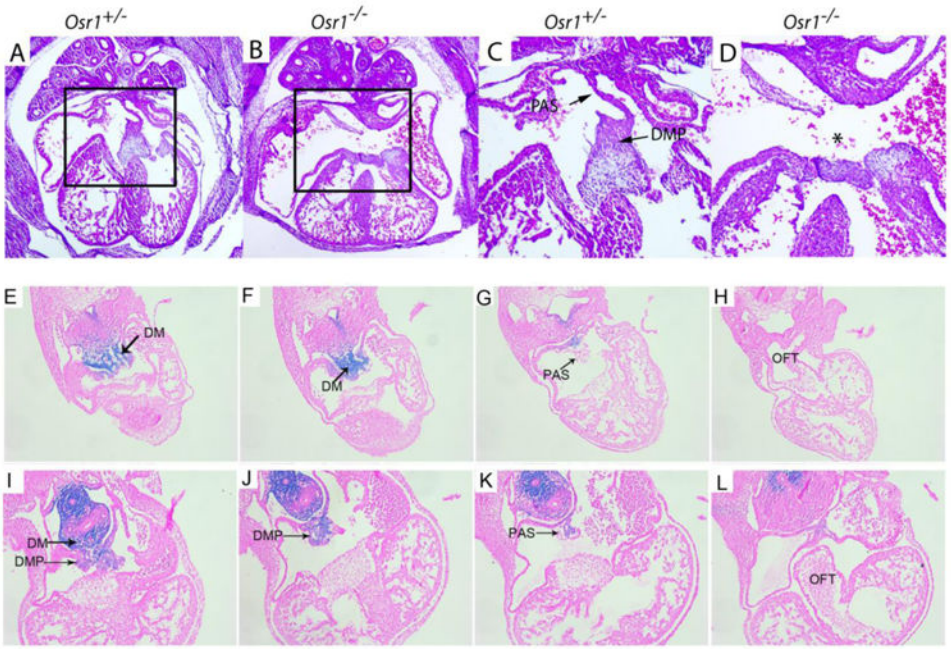

Figure 1. Osr1 is expressed in the dorsal mesocardium and DMP

(A-D) Histology of the *Osr1*$^{-/-}$ embryos that survive through E13.5 and their littermate control. (E-H) Expression of *Osr1* was detected by X-gal staining to reveal the β-galactosidase activity in *Osr1*$^{-/+}$ mouse embryos at E9.5.

(I-L) Expression of *Osr1* was detected by X-gal staining to reveal the β-galactosidase activity in *Osr1*$^{-/+}$ mouse embryos at E10.5.

Magnification in panels A and B, 40×; magnification in panels C and D, 100×; magnification in panels E-L, 200×. The "*" indicates missing of structures of atrial septation. DM, dorsal mesocardium; PAS, primary atrial septum; DMP, dorsal mesenchymal protrusion; OFT, outflow tract

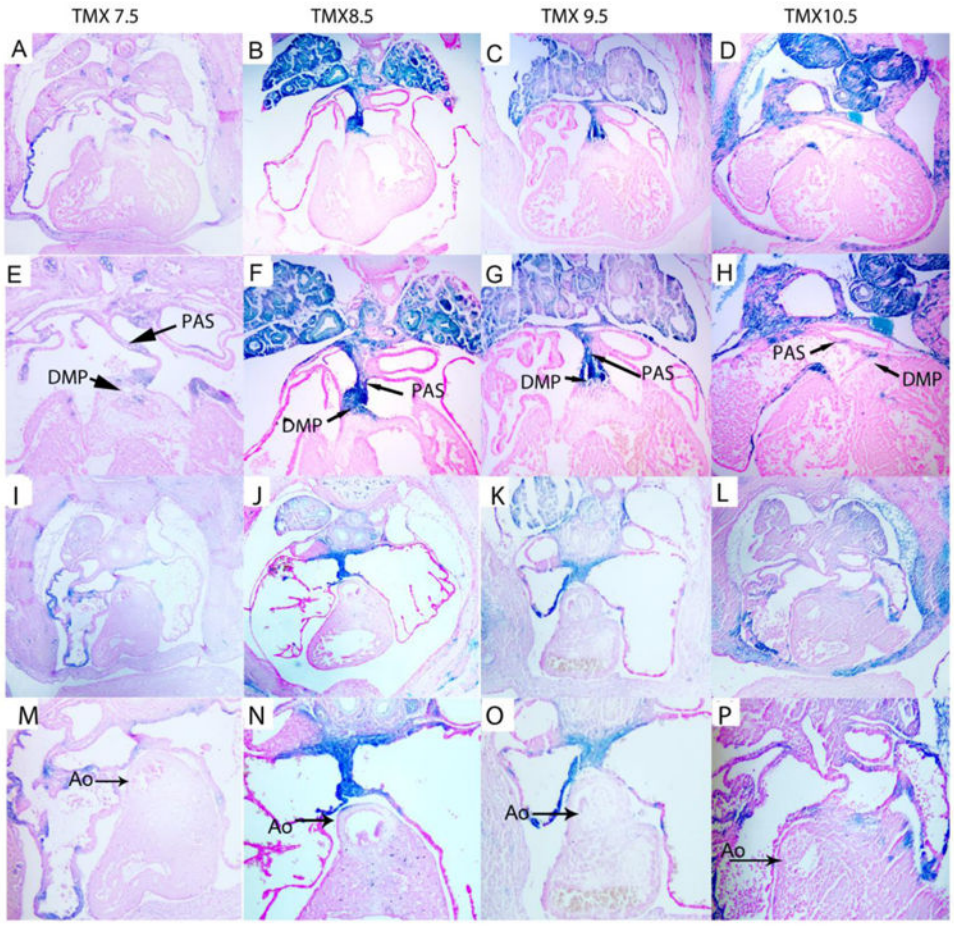

Figure 2. Osr1-expressing cells contribute to the atrial septal structure during E8 to E10.5

Descendant cells of Osr1-positive cells were marked in space and time by using a TM-inducible Cre recombinase expressed from the *Osr1* locus *(Osr1cre:ERT).* Embryos were given TM (75 mg/kg) at E6.5, E7.5 (A, E, I and M), E8.5 (B, F, J and N), E9.5 (C, G, K and O), or E10.5 (D, H, L and P), and β-galactosidase expression was evaluated in $R26R^{Osr1\text{-}CreERT2/+}$ embryos at E13.5. Magnification in panels A-D and I-L, 40×; magnification in panels E-H and M-P, 100×. PAS, primary atrial septum; DMP, dorsal mesenchymal protrusion

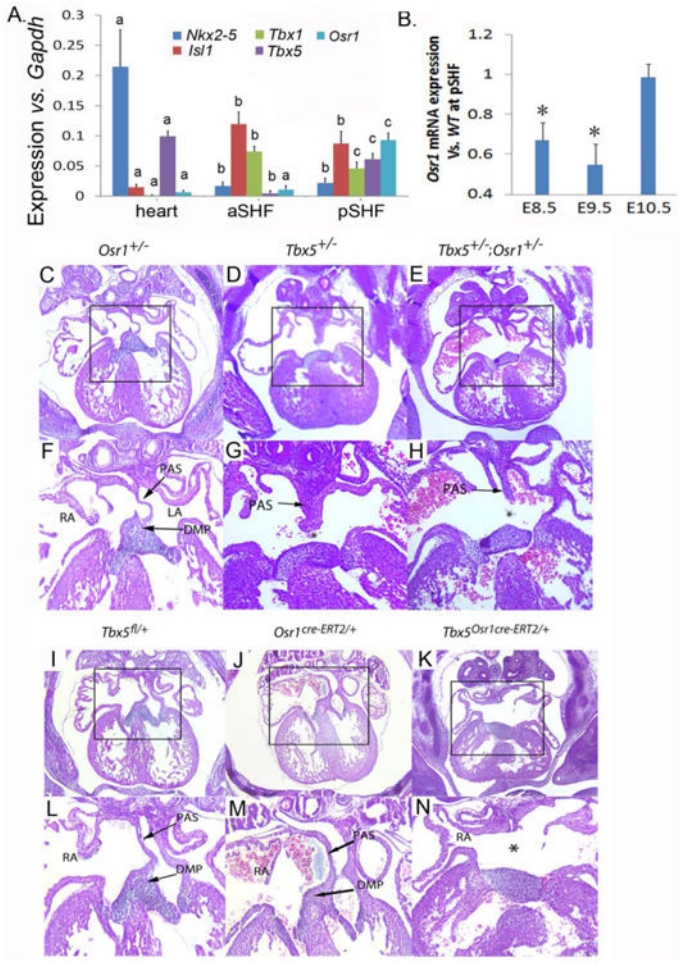

Figure 3. *Osr1* interacts with *Tbx5* in atrial septum progenitors

(A) Expression levels of *Gapdh*, *Nkx2-5*, *Isl1*, *Tbx1*, *Tbx5* and *Osr1* in the micro-dissected heart, pSHF and aSHF of E9.5 *wildtype* mouse embryos were evaluated by real-time PCR analysis. Expression of *Nkx2-5*, *Isl1*, *Tbx1*, *Tbx5* and *Osr1* versus *Gapdh* were calculated by ΔCt method [27]. Significant difference of each gene expression among heart, aSHF and pSHF was tested by ANOVA analysis using ΔCt value. Different letters denote significant difference ($P<0.05$) among heart, aSHF and pSHF.

(B) Expression levels of *Osr1* in the pSHF at E8.5, E9.5, and E10.5 were evaluated by real-time PCR analysis. * $P<0.05$ vs. WT

(C-H) Histology of $Osr1^{+/-}$ (B and E), $Tbx5^{+/-}$ (C and F) and $Tbx5^{+/-}$;$Osr1^{+/-}$ (D and G) at E13.5.

(I-N) Histology of $Tbx5^{Osr1\text{-}CreERT2/+}$ and their littermate control embryos at E13.5. Magnification in panels B-D and H-J, 40×; Magnification in panels E-G and K-M, 100×. *, missing of structures of atrial septation. The "*" indicates missing structures of atrial septation. PAS, primary atrial septum; DMP, dorsal mesenchymal protrusion; RA, right ventricle

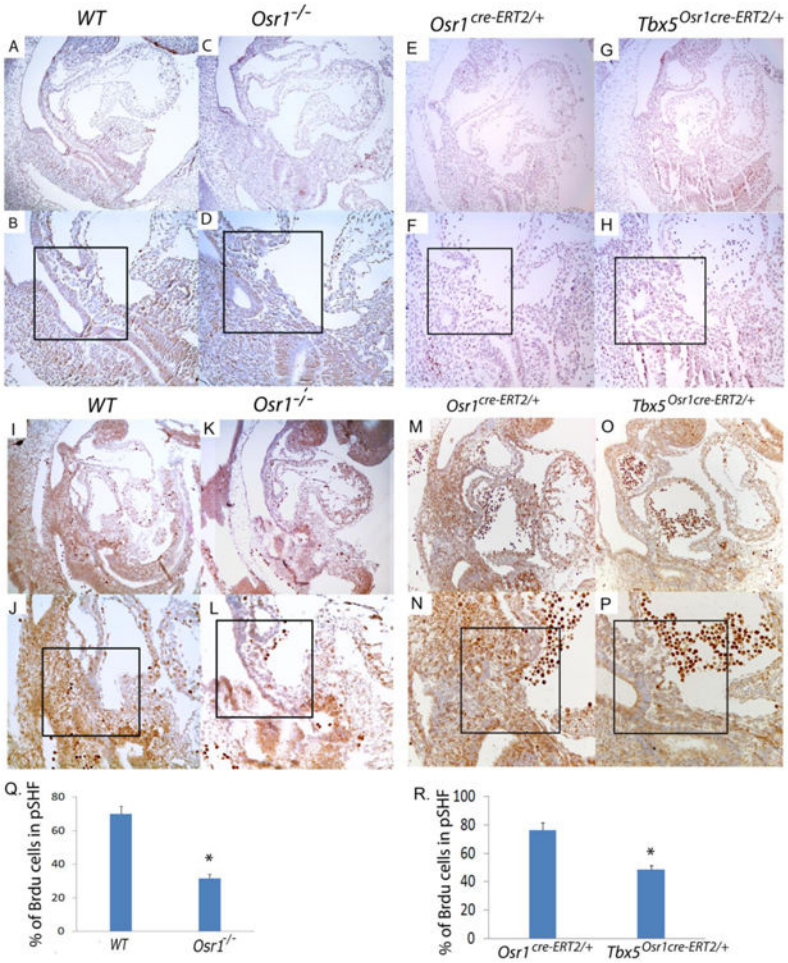

Figure 4. *Osr1* plays an important role in regulating pSHF cardiac progenitors' proliferation

(A-D) Apoptosis within the pSHF of either *Osr1*$^{-/-}$ embryos (A, B) or wild-type littermate control embryos (C, D) was analyzed by TUNEL staining.

(E-H) Apoptosis within the pSHF of either *Tbx5*$^{Osr1cre-ERT2/+}$ (G, H) or *Osr1*$^{Cre-ERT2/+}$ embryos (E, F) was analyzed by TUNEL staining.

(I-L) Proliferating cells within the pSHF of Osr1$^{-/-}$ embryos (I, J) or wild-type littermate control embryos (K, L) was detected by BrdU incorporation.

(M-P) Proliferating cells within the pSHF of either *Tbx5*$^{Osr1cre-ERT2/+}$ (O, P) or *Osr1*$^{Cre-ERT2/+}$ embryos (M, N) was detected by BrdU incorporation.

(Q and R) The ratio of BrdU-positive cardiac progenitors to pSHF cells was calculated within a total of 500 cells (100 cells/section) in the pSHF and the DMP region (an example of a typical region is indicated as the framed areas). The mean values ±SEM (n=3 or 4 embryos) are presented. Difference among treatment groups was tested by one-way analysis of covariance (ANOVA). * $P<0.05$

Magnification in panels A, C, E, G, I, K, M, and O, 100×; magnification in B, D, F, H, J, L, N, and P, 200×.

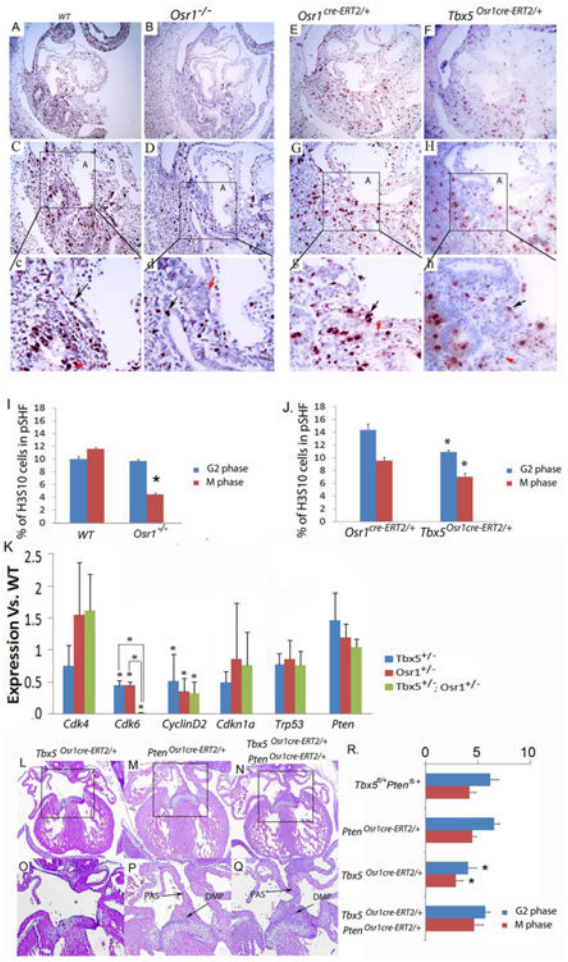

Figure 5. *Tbx5* and *Osr1* interact in regulating the transition from the G1-S phase of pSHF cardiac progenitors

A-D) G2 and M phase cells within the pSHF of either *Osr1*$^{-/-}$ embryos (B, D) or wild-type littermate control embryos (A, C) was detected by immunohistological staining of H3S10. (The black arrow indicates a typical cell in M phase, and the red arrow indicates a typical cell in G2 phase). Enlargement of the framed region are shown in panel c and d.

(E-H) G2 and M phase cells within the pSHF of either *Tbx5*$^{Osr1cre\text{-}ERT2/+}$ (F, H) or *Osr1*$^{Cre\text{-}ERT2/+}$ embryos (E, G) was detected by immunohistological staining of H3S10. (The black arrow indicates a typical cell in M phase, and the red arrow indicates a typical cell in G2 phase). Enlargement of the framed region are shown in panel g and h.

(I and J) The proportion of H3S10-positive cardiac progenitors within a total of 500 cells in the pSHF and the DMP region was calculated (an example of a typical region is shown in c, d, g, and h). Total of five hundred cells (100 cells/section) were counted within the pSHF region of each embryo and percentage of positive cells were calculated. These were repeated on three or four embryos in each treatment groups and difference among treatment groups was tested by ANOVA.

(K) Expression levels of *Cdk4, Cdk6, Cyclin D2, Cdkn1a, Trp53 and Pten* in the pSHF at E9.5 were detected by real-time PCR. Data is expressed as “mean fold change (vs. *wildtype*)

± *SE*" calculated using a ΔΔCt method [27]. Differences among the four groups were analyzed by ANOVA using ΔCt value, *p<0.05, n=3 embryos

(L-Q)Histology of *Pten*$^{Osr1Cre\text{-}ERT2/+}$, *Tbx5*$^{Osr1Cre\text{-}ERT2/+}$; *or Tbx5*$^{Osr1Cre\text{-}ERT2/+}$; *Pten*$^{Osr1\ Cre\text{-}ERT2/+}$ embryos at E14.5.

(R) The proportion of H3S10-positive cardiac progenitors within a total of 500 cells in the pSHF and the DMP region of *Pten*$^{fl/+}$;*Tbx5*$^{fl/+}$, or *Pten*$^{Osr1Cre\text{-}ERT2/+}$, or *Tbx5*$^{Osr1Cre\text{-}ERT2/+}$; *or Tbx5*$^{Osr1Cre\text{-}ERT2/+}$; *Pten*$^{Osr1Cre\text{-}ERT2/+}$ embryos was calculated. Total of five hundred cells (100 cells/section) were counted within the pSHF region of each embryo and percentage of positive cells were calculated. These were repeated on three or four embryos in each treatment groups and difference among treatment groups was tested by one-way analysis of covariance (ANOVA). Magnification in panels A, B, E, and F, 100×; magnification in panels C, D, G, and H, 200×, magnification in panels c, d, g, and h, 400×; magnification in panels M-R, 40×. PAS, primary atrial septum; DMP, dorsal mesenchymal protrusion; A, atrium

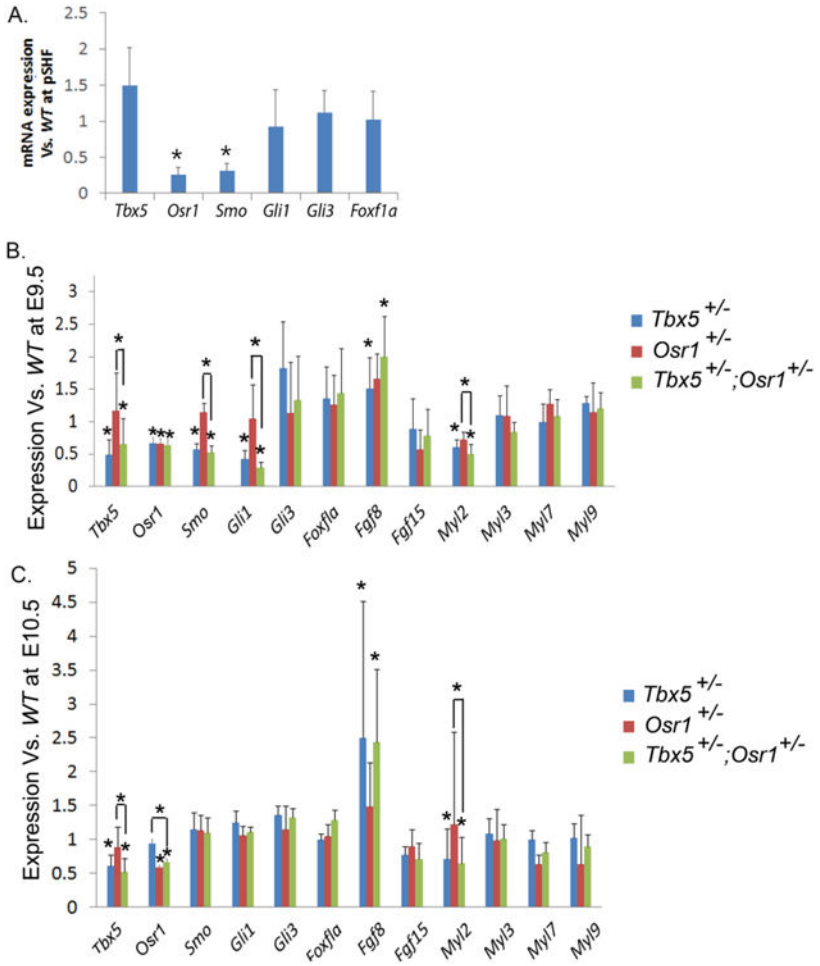

Figure 6. Hh signaling was differentially regulated in the pSHF at E9.5 and E10.5

(A) Expression levels of *Tbx5, Osr1, Smo, Gli, Gli3 and Foxf1a* in the pSHF at E9.5 were detected by real-time PCR. Data is expressed as "mean fold change (vs. *wildtype*) ± *SE*" *calculated using a* ΔΔCt method [27]. Differences among the four groups were analyzed by ANOVA using ΔCt value, *p<0.05, n=3 embryos

(B and C) Heart related gene expression in the pSHF at E9.5 (B) and E10.5 (C) were detected by real-time PCR. Data is expressed as "mean fold change (vs. *wildtype*) ± *SE*" *calculated using a* ΔΔCt method[27]. Differences among the four groups were analyzed by ANOVA using ΔCt value, *p<0.05, n=3 embryos

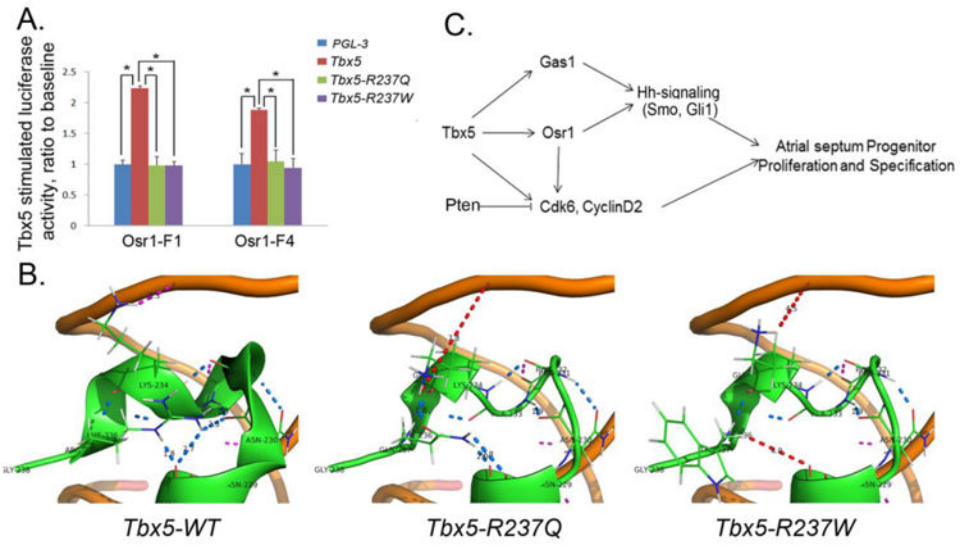

Figure 7. Mutation of Tbx5 blocked Osr1 transactivation, which might be associated with lower binding stability between Tbx5 and DNA strand

A) Luciferase reporter assay was carried out to test if point mutation of Tbx5 failed to transactivate Osr1 through known Osr1 promoter region (Osr1-F1 and Osr1-F4). Data are presented as mean ± SEM, n=3.

B) Structure differences between Tbx5 and the Tbx5 mutants. Hydrogen bond between DNA strand (in light brown) and Tbx5 protein (in green) is indicated by purple dashed line, H-bonds within interested region including 310-helix are shown as blue dashed line. The distance between atoms used to form an H-bond is indicated by red dashed line.

C) Working model for Tbx5 and Osr1 interaction in atrial septation at before E10.5. Tbx5 directly activating Osr1, which impacts on the Hh signaling by regulating the expression levels of *Smo* and *Gli1*. Tbx5 also plays upstream of Osr1 on regulating the cell cycle gene *Cdk6* and *Cycline D2* expression. *Pten*, plays in a parallel pathway of Tbx5 and Osr1 to control the proliferation of atrial septal progenitors.

Table 1

Primers used for RT-PCR

	Forward	Reverse
Cdk4	5′-GCTCGCGGCCTGTGTCTAT-3′	5′-CCATTCTCGAAGCAGGGGAT-3′
Cdk6	5′-TCACGGACGGACAGAGAAAC-3′	5′-GCCGGGCTCTGGAACTTTAT-3′
Cdk5r2	5′-TCGTTCACCCTTTCCGTCTG-3′	5′-GGTGGACTTTGAGATGCCCA-3′
Cdkn1a	5′-CGGTGTCAGAGTCTAGGGGA-3′	5′-AGGATTGGACATGGTGCCTG-3′
Cyclin D2	5′-GCCAAGATCACCCACACTGA-3′	5′-GCGTTATGCTGCTCTTGACG-3′
Tbx5	5′-GCTCCCAGCAAGTCTCCATC-3′	5′-TTCGTGGAACTTCAGCCACA-3′
Osr1	5′-GTGACCAAGCTATCCCCAGA-3′	5′-CCACAGAACTTGCAAACGAA-3′
Smo	5′-GCTGAAGGTGATGAGCACAA-3′	5′-CAGCAAGATCAACGAGACCA-3′
Gli1	5′-GCCTTGAAAACCTCAAGACG-3′	5′-ATGGCTTCTCATTGGAGTGG-3′
Gli3	5′-ACCCTGCTGCTCTGACTCAT-3′	5′-GCAACCTCACTCTGCAACAA-3′
Foxfla	5′-GCTCAACGAGTGCTTCATCA-3′	5′-CGCATCGATGGTCCAGTAGT-3′
Fgf8	5′-GCGGGTAGTTGAGGAACTCG-3′	5′-GTACATGGCCTTTACCCGGA-3′
Fgf15	5′-TGAGCCATCCAGTTGTGTCC-3′	5′-CCACTGGAGAATTTGGGGCT-3′
Myl2	5′-GAAGGACTGAGCCCTGAACC-3′	5′-TGTTTATTTGCGCACAGCCC-3′
Myl3	5′-AGCCCAAGAAGGATGATGCC-3′	5′-AGGCATCAAACTCGGCTTCC-3′
Myl7	5′-GCTCGGGAGGGTAAGTGTTC-3′	5′-GTCCCATTGAGCTTCTCCCC-3′
Myl9	5′-GCCAAGGACAAGGACGACTAA-3′	5′-CTAATTCGTCACGGGGAGGG-3′

Table 2

Incidence of ASDs in embryos.

(A)Knockout of *Osr1*				
Genotype	AVSD	Total	P value(χ^2 test)	
Osr1$^{-/-}$	9	12	*Osr1*$^{-/-}$(9/12):*WT*(0/10) *Osr1*$^{-/-}$(9/12):*Osr1*$^{+/-}$ (0/10)	P=0.000367 P=0.000367
(B) *Tbx5 – Osr1* compound mutant embryos				
Tbx5$^{+/-}$;*Osr1*$^{+/-}$	11	11	*Tbx5*$^{+/-}$;*Osr1*$^{+/-}$(11/11):*Osr1*$^{+/-}$(0/8) *Tbx5*$^{+/-}$;*Osr1*$^{+/-}$(11/11):*Tbx5*$^{+/-}$(5/10)	P=0.001 P=0.0149
Tbx5$^{Osr1cre\text{-}ERT2/+}$	7	11	*Tbx5*$^{Osr1cre\text{-}ERT2/+}$(7/11):*Tbx5* $^{fl/+}$(0/7) *Tbx5*$^{Osr1cre\text{-}ERT2/+}$(7/11):*Osr1*$^{cre\text{-}ERT2/+}$(0/7)	P=0.0138 P=0.0138
(C) Effect of TMX administration on ASD in *Tbx5* $^{Osr1cre\text{-}ERT2/+}$ *embryos.*				
Tbx5$^{Osr1cre\text{-}ERT2/+}$ (TMX 8.5;9.5)	9	11	*Tbx5* $^{Osr1cre\text{-}ERT2/+}$(TMX 8.5;9.5) (9/11): *Tbx5* $^{Osr1cre\text{-}ERT2/+}$(TMX 7.5;8.5) (7/11):	P=0.3161
(D) *Pten – Tbx5 – Osr1* compound mutant embryos				
Tbx5$^{Osr1cre\text{-}ERT2/+}$;*Pten*$^{osr1cre\text{-}ERT2/+}$	1	6	*Tbx5*$^{Osr1cre\text{-}ERT2/+}$;*Pten*$^{Gli1ERT2\text{-}Cre/+}$(1/6): *Tbx5*$^{Osr1cre\text{-}ERT2/+}$(8/12) *Tbx5*$^{Osr1cre\text{-}ERT2/+}$;*Pten*$^{Gli1ERT2\text{-}Cre/+}$(1/6): *Pten*$^{Osr1cre\text{-}ERT2/+}$(0/7)	P=0.0062 P=0.2038

* Incidence of AVSDs was evaluated in mutant embryos at E13.5. Significance in AVSD incidence between mutant embryos and littermate controls was analyzed by the χ^2 test.